How Colors Influence Numbers: Photon Statistics of Parametric Downconversion

Wolfgang Mauerer,* Malte Avenhaus, Wolfram Helwig, and Christine Silberhorn
Max Planck Research Group, Institute of Optics,
Information and Photonics, Junior Research Group IQO
(Dated: November 6, 2018)

Parametric downconversion (PDC) is a technique of ubiquitous experimental significance in the production of non-classical, photon-number correlated twin beams. Standard theory of PDC as a two-mode squeezing process predicts and homodyne measurements observe a thermal photon number distribution per beam. Recent experiments have obtained conflicting distributions. In this paper, we explain the observation by an *a-priori* theoretical model solely based on directly accessible physical quantities. We compare our predictions with experimental data and find excellent agreement.

PACS numbers: 42.50.Ar 89.60.Gg

Introduction Spectral properties of states generated by $\chi^{(2)}$ nonlinearities are traditionally studied using homodyne detection. Unfortunately, this standard technique implicitly restricts the observation to an effective single spectral mode imposed by the single local oscillator. Avalanche photo diodes (APDs) [1], in contrast, are sensitive on all modes generated by sources of current experimental significance, and uncover richer spectral properties. This sub-structure is currently usually neglected or only treated effectively, although it impacts security proofs of quantum key distribution or the validity of fundamental quantum measurements, for example.

In this paper, we present an *a-priori* theoretical explanation that connects the spectral structure of PDC states with the photon number distribution (PND), which is a commonly employed resource. Recent experiments have observed that the PND for multi-mode sources differs markedly from the prediction of the single-mode standard model [2]. Our approach explains this behavior by decomposing the state into a set of independent two-mode squeezers [3, 4] akin, but not completely identical to the Bloch-Messiah decomposition. The PND is inferred from the well-known properties of these independent contributions. In contrast to previous efforts [5, 6], our approach is the first to enable, to our knowledge, the quantitative computation of photon number statistics *without* assumptions or fitting of non-physical parameters. This is important for a wide class of experiments ranging from fundamental to highly applied because they require a complete understanding of the internal structure of PDC states to fully exploit their quantum features.

Decomposition A multi-mode type-II downconversion process is most conveniently studied using the interaction Hamiltonian $\hat{H}_{\mathrm{int}}(t) = \int_V \mathrm{d}^3\vec{x}\chi^{(2)}\hat{E}_p^{(+)}(\vec{x},t)\hat{E}_s^{(-)}(\vec{x},t)\hat{E}_i^{(-)}(\vec{x},t) + \mathrm{H.c.}$ [7], where the subscripts denote pump, signal, and idler, respectively, and the tensor $\chi^{(2)}$ represents the second-order nonlinear susceptibility. By assuming a classical pump and a frequency-independent $\chi^{(2)}$ in the spectral range of interest, it can be shown [8] that with $\hat{H}_I \equiv \int_{t_0}^{t} \mathrm{d}t' \hat{H}_{\mathrm{int}}(t')$,

$$\hat{H}_I = C \iint \mathrm{d}\omega_1 \mathrm{d}\omega_2 f(\omega_1,\omega_2)\hat{a}^\dagger(\omega_1)\hat{b}^\dagger(\omega_2) + \mathrm{H.c.}, \quad (1)$$

where $\hat{a}^\dagger(\omega_1)$ and $\hat{b}^\dagger(\omega_2)$ are field operators that create a monochromatic photon with frequency ω_i in the signal and idler modes a and b. $f(\omega_1,\omega_2)$ is the spectral distribution function (SDF) of the single photon contribution, and $C = C(\chi^{(2)}, \sqrt{I_p})$ is a coupling constant that depends on the strength $\chi^{(2)}$ of the nonlinear susceptibility and on the pump intensity [7, 9]. The time-propagated state is computed by $|\psi\rangle = \mathcal{T}\exp((i\hbar)^{-1}\hat{H}_I)|\psi(t_0)\rangle$, where we assume that the pulse has completely left the crystal and the interaction is finished. Following [8], the time-ordering $\mathcal{T}$ can be omitted because the Hamiltonian approximately commutes with itself at different times and the corrections are therefore negligible.

To express $\hat{H}_I$ in a more convenient form, we use the Schmidt decomposition, uniquely defined by

$$f(\omega_1,\omega_2) = \sum_{n=0}^{N-1} \sqrt{\lambda_n}\xi_n^{(1)}(\omega_1)\xi_n^{(2)}(\omega_2), \quad (2)$$

where the Schmidt modes $\{\xi_n^{(1)}(\omega_1)\}$ and $\{\xi_n^{(2)}(\omega_2)\}$ are two sets of orthonormal bases with respect to the L^2 inner product, and the Schmidt eigenvalues λ_n are real expansion coefficients that satisfy $\sum_n \lambda_n = 1$. The salient feature of Eq. (2) is that only a single summation index is required, and not two as for a regular change of basis. The decomposition is guaranteed to exist for a large class of systems under very general assumptions [10]. For simple systems that require only a few Schmidt modes (*i.e.*, N is small), the decomposition can be numerically computed by solving a set of coupled integral equations [11]. For systems that require a large N, it is usually easier to perform a singular value decomposition (SVD), see Ref. [12] and below for more details.

We define effective single-mode field operators (sometimes also called pseudo-boson operators) by

$$\hat{A}_n^\dagger \equiv \int \mathrm{d}\omega \xi_n^{(1)}(\omega)\hat{a}^\dagger(\omega), \quad (3)$$

and similarly for $\hat{B}_n$. Because the spectral distribution functions are orthonormal, that is, $\langle \xi_i, \xi_j \rangle = \delta_{ij}$, it is easy to verify that the operators fulfill the canonical commutation relations $[\hat{A}_j, \hat{A}_k^\dagger] = \hat{\mathbb{1}}\delta_{jk}$ and $[\hat{A}_j, \hat{A}_k] = 0$. More details about this notation are provided by Ref. [13].

By rewriting $\hat{H}_I$ in Eq. (1) using the Schmidt decomposition (2) for $f(\omega_1, \omega_2)$ and the definition of pseudo-boson operators in Eq. (3), we obtain

$$\exp\left(\frac{1}{i\hbar}\hat{H}_I\right) = \exp\left(\frac{C}{i\hbar}\sum_{n=0}^{N-1}\sqrt{\lambda_n}\hat{A}_n^\dagger\hat{B}_n^\dagger + \text{H.c.}\right). \quad (4)$$

The two-mode squeezing operator for spectral effective single modes A, B is defined by $\hat{S}_{\text{AB}}(\eta_n) \equiv \exp(-\eta_n\hat{A}^\dagger\hat{B}^\dagger + \eta_n^*\hat{A}\hat{B})$, where $\eta_n = C\sqrt{\lambda_n}/(i\hbar) \equiv r_n \exp i\varphi_n$ is a complex number. Because $[\hat{A}_j, \hat{A}_k^\dagger] = 0$ for $j \neq k$, the state after the interaction is a tensor product of independent two-mode squeezers[21]:

$$|\psi\rangle = \bigotimes_{n=0}^{N-1}\hat{S}_{A_nB_n}(\eta_n)|\psi(t_0)\rangle. \quad (5)$$

Notice that it follows from this decomposition that the SDF is identical for all orders of photon number contributions because creation operators that belong to different distribution functions are never mixed.[22]

Computing Statistical Distributions For two-mode squeezed states, the PND in each mode is thermal, that is, for the state

$$|\psi\rangle = \hat{S}_{AB}(\eta)|00\rangle = \sum_{n=0}^{\infty}\kappa_n|n,n\rangle, \quad (6)$$

the distribution is given by $p(n) = |\kappa_n|^2 = \operatorname{sech}^2 r \tanh^{2n} r$ for one output mode, that is, $N = 1$. Consequently, the photon number distribution of the multi-mode state (5) is given by the convolution of the distributions of all independent squeezers. Assume that $p_{\xi_k}(n)$ denotes the PND of the kth squeezer with spectral modes $\xi_k^{(i)}$. The overall PND is then given by

$$p_{\bar{\xi}}(n) = \sum_{\Theta\in n\vdash N}\prod_{m=0}^{N-1}p_{\xi_m}(\Theta_m), \quad (7)$$

where $n \vdash N$ denotes the set of all partitions of n into N parts. The distribution $p_{\bar{\xi}}(n)$ is consequently the convolution of all probability distributions $p_{\xi_i}(n)$.

Two special cases follow directly from Eq. (7): When only a single effective mode contributes ($N = 1$), the resulting distribution exhibits thermal behavior. When the physical process requires a very large number of effective modes ($N \to \infty$), the resulting PND is Poissonian, because it is known that a convolution of thermal distributions converges to a Poissonian distribution in this limit [14].

Computing the convolution in Eq. (7) involves summing over numerous contributions. This is considerably simplified by using generating functions. For coefficients $p(n)$, they are given by the formal power series [14] $g(\zeta) = \sum_n p(n)\zeta^n$. The individual coefficients can be recovered via $p(n) = \frac{1}{n!}\frac{\partial^n}{\partial x^n}\, g(\zeta)|_{\zeta=0}$. For the thermal distribution of a two-mode squeezer, the series converges analytically to $g_k(\zeta) = \frac{\operatorname{sech}^2 r_k}{1-\zeta\tanh^2 r_k}$, where r_k is the strength of the kth squeezer. The generating function for a convolution of N thermal distributions is $\prod_{k=0}^{N-1} g_k(\zeta)$, and the resulting photon number distribution is consequently

$$p_{\bar{\xi}}(n) = \frac{1}{n!}\left(\frac{\partial^n}{\partial\zeta^n}\prod_{k=0}^{N-1}g_k(\zeta)\right)\bigg|_{\zeta=0}. \quad (8)$$

Let us now turn our attention to an example illustrating our considerations. Assume that the SDF is given by a two-dimensional, real-valued Gaussian distribution (this is not a restriction because the methods also work for complex, non-Gaussian SDFs). This approximation is commonly used [11, 15] to provide a convenient parameterization of type-II PDC processes. Especially, it is possible to perform an analytical Schmidt decomposition (a similar approach is used, for instance, in Ref. [15]). We use the parameters σ_x^2 and σ_y^2 to specify the spectral widths of signal and idler, while θ denotes the rotation with respect to the x axis. This form is illustrated in Figure 3.

Let us choose $\sigma_x^2 = 25$ and $\sigma_y^2 = 1$, which are the parameters depicted in the inset of Figure 3. The Schmidt number $K = 1/\sum_n \lambda_n^2$ is computed from the eigenvalues λ_n of the Schmidt decomposition. It is a measure for the number of effectively contributing spectral modes and thus of inherent spectral correlations of the physical process [11] (notice that we could have also considered an entanglement monotone like the logarithmic negativity for this purpose). For $\theta = 0$, the state exhibits no spectral correlations, and a single Schmidt mode suffices for the decomposition. By rotating the SDF from $\theta = 0$ to $\theta = \pi/2$, the correlations increase to their maximal value at $\theta = \pi/4$, and decrease again until the SDF becomes separable for $\theta = \pi/2$. This implies thermal statistics for $\theta = 0$ and $\theta = \pi/2$, and maximal similarity to Poissonian statistics for $\theta = \pi/4$. The coupling and pump intensity are, for better comparability, chosen such that $\bar{n} = 1$ for all PNDs. Figure 1 illustrates the arising distributions.

To quantify the difference between convoluted and Poissonian or thermal distributions, we employ the variational distance defined for two probability distributions p_1, p_2 as $\Delta_{p_1,p_2} \equiv \sum_n |p_1(n) - p_2(n)|$. Two distributions are completely identical if and only if $\Delta = 0$. Figure 2 compares the difference of the convoluted distribution to the above-mentioned special cases for a growing Schmidt number K, that is, a growing number of Schmidt modes achieved by rotating the Gaussian SDF for $\theta = 0$ to $\theta = \pi/4$.

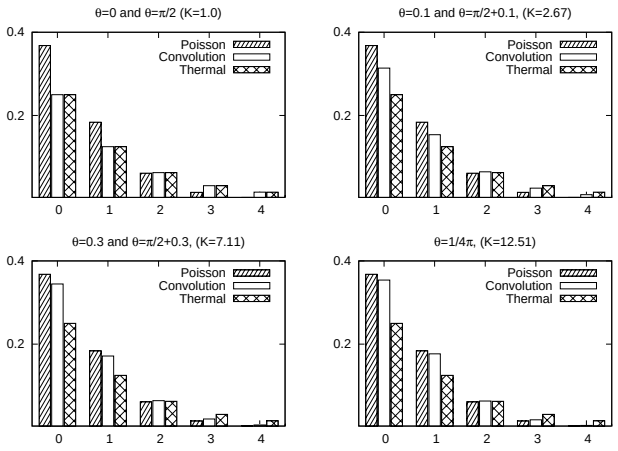

FIG. 1: Photon number distribution depending on the number of effectively contributing modes as given by the Schmidt number K (and thus on the angle of the SDF) of a type-II PDC process. The x axes depict photon numbers, whereas the y axes show probabilities.

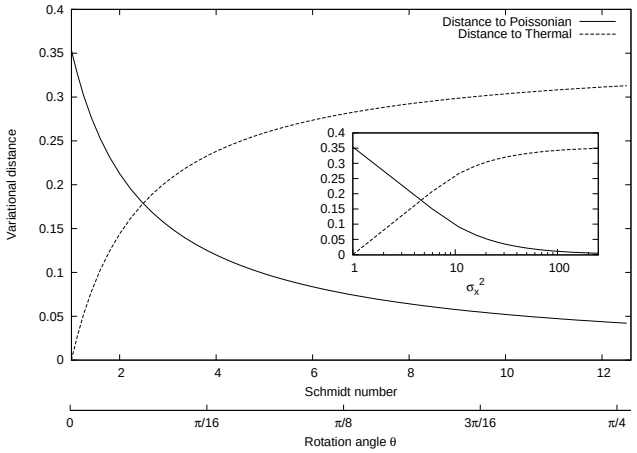

FIG. 2: Solid line and dashed line show the distance between the convoluted photon-number distribution and Poissonian or thermal statistics, respectively, plotted against Schmidt number. For a single effective mode, the distribution is exactly thermal, but the more modes contribute, the closer it gets to a Poissonian distribution. The inset fixes $\theta = \pi/4$ and varies σ_x^2, which is drawn on a logarithmic scale.

Once again, we emphasize that the shift towards a Poissonian distribution is inherent in the physical process and not caused by any experimental imperfections.

Comparison with Experimental Data We have also performed a comparison of experimentally measured photon number statistics with the predictions of our theory. A photon-number resolving fiber-loop detector [1] in combination with highly efficient waveguides was used to record the distribution. The detection method is resilient against loss and allows us to eliminate the corresponding effects when ensemble measurements are performed. Ref. [12] shows the experimental details of state generation, and [2] describes the measurement procedure. Figure 3 compares the experimentally observed distribution with the theoretical prediction at various pump powers. As is immediately obvious from the figure, they are in excellent agreement.

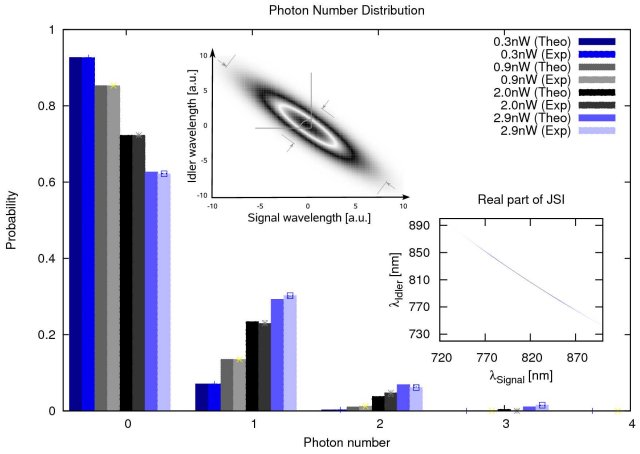

FIG. 3: (Color online) Comparison between experimentally measured and theoretically obtained photon number distributions for a multi-mode PDC process at various pump strengths. The bottom inset shows the real part of the joint spectral intensity, while the top inset demonstrates the parameterization of the analytical Gaussian approximation of the SDF. Loss inversion and error estimation was performed using non-negative least squares optimization.

To avoid the necessity of fitting any effective parameters, we have obtained an exact numerical decomposition using SVD techniques. After discretizing the SDF on a grid M_{mn} of size 1500×1500, the matrix is decomposed as $M = U\Sigma V^\dagger$, where U, V are unitaries and $\Sigma = \mathrm{diag}(\sqrt{\lambda_1}, \ldots, \sqrt{\lambda_N})$ is a real diagonal matrix [16]. Extensive checks that the decomposition converges (and also converges to the proper value) have been performed, see Ref. [17] for details.

Notice that the decomposition of the spectral distribution does *not* depend on the pump intensity, which means that the composition $\{\lambda_n\}$ of the PND is fixed for the physical process. However, the observed *mean value* of the PND does depend on the pump intensity, and Fig. 3 shows a shift toward larger mean photon numbers for larger pump intensities as expected.

For higher pump powers, photon-number resolved detection is not possible anymore. To check the theory in this regime, we have used a set of mean photon number ($\bar{n}$) measurements instead. The coupling constant C as defined in Eq. 1 can be inferred from the decomposed SDF for each $\bar{n}$ for a given pump power by a numerical optimization process[23]. The result is shown in Figure 4. Again, very good agreement between theory and experiment is achieved.

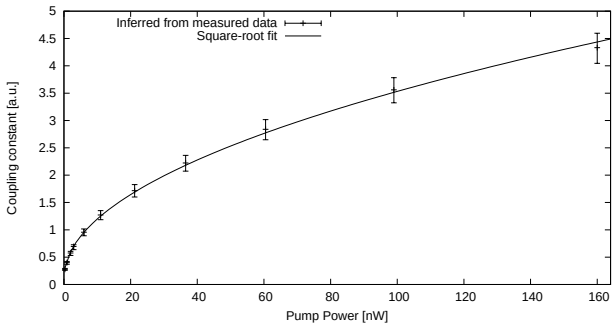

FIG. 4: Relation between pump power and coupling parameter. The expected square-root dependency [9] is correctly obtained for a wider range of pump intensities than can be resolved with current TMDs, which ensures the validity of our approach also for high powers. Notice that this knowledge would also allow for computing the expected mean photon number for a given pump power or a determination of $\chi^{(2)}$, as described in [18].

Conclusions We have shown how to decompose a multi-mode PDC process into independent two-mode squeezers operating on effective single modes, and how this explains why the photon number distribution of the process can exhibit any form ranging from purely thermal to purely Poissonian. We have underlined the validity of the theory by comparing the predictions to an experimentally measured photon number distribution. Additionally, we have compared theory and experiment for larger pump powers.

Appendix A two-dimensional Gaussian distribution in a suitable parameterization is given by

$$\begin{aligned} f(x,y) &= \frac{1}{\sqrt{\pi\sigma_x\sigma_y}}\exp(-ax^2-2bxy-cy^2),\\ a(\theta,\sigma_x,\sigma_y) &= \cos^2\theta/(2\sigma_x^2)+\sin^2\theta/(2\sigma_y^2),\\ b(\theta,\sigma_x,\sigma_y) &= -\sin 2\theta/(4\sigma_x^2)+\sin 2\theta/(4\sigma_y^2),\\ c(\theta,\sigma_x,\sigma_y) &= \sin^2\theta/(2\sigma_x^2)+\cos^2\theta/(2\sigma_y^2). \end{aligned}$$

Without getting into details of the algebra involved, we remark that by starting from Mehler's formula [20] $\sum_{n=0}^{\infty} H_n(x)H_n(y)\frac{(\frac{1}{2}\gamma)^n}{n!} = \frac{1}{\sqrt{1-\gamma^2}}\exp\left(-\frac{\gamma^2x^2-2\gamma xy+\gamma^2y^2}{1-\gamma^1}\right)$ ($H_n(x)$ denotes the Hermite polynomial of nth order), it is possible to bring $f(x,y)$ into the form $f(x,y)=\sum_{n=0}^{\infty}\sqrt{\lambda_n}f_n^{(1)}(x)f_n^{(2)}(y)$. The coefficients λ_n are given by $\lambda_n = \frac{2^{2n-1}}{ac}\frac{1+\gamma^2}{\sigma_x\sigma_y}\left(\frac{\gamma}{2}\right)^{2n}$ where $\gamma=\frac{-2\sqrt{ac}+\sqrt{4ac-4b^2}}{2b}$. Since the set $\{\lambda_n\}$ contains all information required for our calculations, the exact form of $f_n^{(i)}(\cdot)$ is not of interest here, but can be found in Ref. [18].

This work was supported by the EC under the FET-Open grant agreement CORNER, number FP7-ICT-213681.

* Electronic address: wolfgang.mauerer@ioip.mpg.de

[1] D. Achilles, C. Silberhorn, C. Sliwa, K. Banaszek, and I. A. Walmsley, Optics Letters **28**, 2387 (2003).
[2] M. Avenhaus, H. B. Coldenstrodt-Ronge, K. Laiho, W. Mauerer, I. A. Walmsley, and C. Silberhorn, Phys. Rev. Lett. **101**, 053601 (2008).
[3] S. L. Braunstein, Phys. Rev. Lett. **71**, 055801 (2005).
[4] W. Wasilewski, A. I. Lvovsky, K. Banaszek, and C. Radzewicz, Physical Review A **73**, 063819 (2006).
[5] J. Perina Jr, O. Haderka, and M. Hamar, arXiv:quant-ph/0310065 (2003).
[6] W. Wasilewski, C. Radzewicz, R. Frankowski, and K. Banaszek, arXiv/0805:1701 (2008).
[7] F. Dell'Anno, S. De Siena, and F. Illuminati, Physics Reports **428**, 53 (2006).
[8] W. P. Grice and I. A. Walmsley, Phys. Rev. A **56**, 1627 (1997).
[9] M. I. Kolobov, Rev. Mod. Phys. **71**, 1539 (1999).
[10] S. Parker, S. Bose, and M. B. Plenio, Physical Review A **61**, 32305 (2000).
[11] C. K. Law, I. A. Walmsley, and J. H. Eberly, Phys. Rev. Lett. **84**, 5304 (2000).
[12] M. Avenhaus, M. V. Chekova, L. Krivitski, G. Leuchs, and C. Silberhorn, arXiv **101**, 0810:0998 (2008).
[13] P. P. Rohde, W. Mauerer, and C. Silberhorn, New Journal of Physics **9**, 91 (2007).
[14] L. Mandel and E. Wolf, *Optical Coherence and Quantum Optics* (Cambridge University Press, 1995).
[15] A. B. U'Ren, K. Banaszek, and I. A. Walmsley, Quant. Inf. & Comp. **3**, 480 (2003).
[16] G. H. Golub and C. F. V. Loan, *Matrix Computations* (Baltimore, MD, USA, 1989), 2nd ed.
[17] W. Mauerer, M. Avenhaus, and C. Silberhorn, to appear in J. Las. Phys. (2009).
[18] W. Mauerer, *PhD thesis* (2009).
[19] S. M. Barnett and P. M. Radmore, *Methods in Theoretical Quantum Optics* (Clarendon Press, 1997).
[20] G. Doetsch, Mathematische Zeitschrift **32**, 587 (1930).
[21] By re-coupling (neglecting unimportant phases) $\hat{A}_j \to 1/\sqrt{2}(\hat{C}_j-\hat{D}_j)$, $\hat{B}_j \to 1/\sqrt{2}(\hat{D}_j+\hat{C}_j)$, it follows that $\hat{S}_{A_jB_j}(\eta)=\hat{S}_{C_j}(\eta)\otimes\hat{S}_{D_j}(\eta)$, that is, a product of two independent effective single-mode squeezers [19]. Using this transformation, we obtain the standard Bloch-Messiah decomposition (see, e.g., Refs. [3, 4]). Owing to the coupling of the signal mode A_j with the idler mode B_j, this form delivers the joint photon number distribution for signal and idler, $p_{\text{joint}}(n)$. It is connected to our distribution via $p_{\text{joint}}(2n)=p(n)$, and $p_{\text{joint}}(2n+1)=0$. When a degenerate PDC process (including type-I) with $\hat{A}_j=\hat{B}_j$ is considered, the decomposition in Eq. (4) automatically leads to the Bloch-Messiah decomposition.
[22] This property can already be inferred from Eq. 4 by defining the operators $\hat{K}_n^{(+)}\equiv\hat{A}_n^\dagger\hat{B}_n^\dagger$, $\hat{K}_n^{(-)}\equiv\hat{A}_n\hat{B}_n$, and $\hat{K}_n^{(0)}\equiv 1/2(\hat{A}_n^\dagger\hat{A}_n+\hat{B}_n^\dagger\hat{B}_n)$ that share the commutation relations $[\hat{K}_n^{(0)},\hat{K}_n^{(\pm)}]=\pm\hat{K}_n^{(\pm)}$ and $[\hat{K}_n^{(-)},\hat{K}_n^{(+)}]=\hat{K}_n^{(0)}$ of an $\mathfrak{su}(1,1)$ Lie algebra, which allows us to apply a specific exponential operator disentangling formula [19, A5.18] from which the desired property is readily derived.
[23] If $\chi^{(2)}$ were known precisely, the optimization would not be necessary